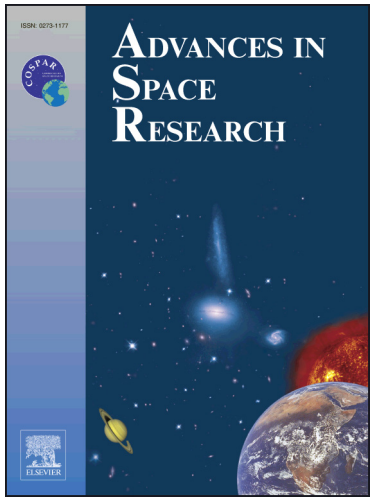

Impact of tracking loop settings of the Swarm GPS receiver on gravity field recovery

C. Dahle, D. Arnold, A. Jäggi

PII: S0273-1177(17)30176-X
DOI: http://dx.doi.org/10.1016/j.asr.2017.03.003
Reference: JASR 13137

To appear in: *Advances in Space Research*

Received Date: 23 December 2016
Revised Date: 24 February 2017
Accepted Date: 4 March 2017

Please cite this article as: Dahle, C., Arnold, D., Jäggi, A., Impact of tracking loop settings of the Swarm GPS receiver on gravity field recovery, *Advances in Space Research* (2017), doi: http://dx.doi.org/10.1016/j.asr.2017.03.003

Impact of tracking loop settings of the Swarm GPS receiver on gravity field recovery

C. Dahle[a,b,*], D. Arnold[b], A. Jäggi[b]

[a] *GFZ German Research Centre for Geosciences, Telegrafenberg, D-14473 Potsdam, Germany*
[b] *Astronomical Institute, University of Bern (AIUB), Sidlerstrasse 5, CH-3012 Bern, Switzerland*

Abstract

The Swarm mission consists of three identical satellites equipped with GPS receivers and orbiting in near-polar low Earth orbits. Thus, they can be used to determine the Earth's gravity field by means of high-low satellite-to-satellite tracking (hl-SST). However, first results by several groups have revealed systematic errors both in precise science orbits and resulting gravity field solutions which are caused by ionospheric disturbances affecting the quality of Swarm GPS observations. Looking at gravity field solutions, the errors lead to systematic artefacts located in two bands north and south of the geomagnetic equator. In order to reduce these artefacts, erroneous GPS observations can be identified and rejected before orbit and gravity field processing, but this may also lead to slight degradations of orbit and low degree gravity field coeffcient quality. Since the problems were believed to be receiver-specific, the GPS tracking loop bandwidths onboard Swarm have been widened several times starting in May 2015. The influence of these tracking loop updates on Swarm orbits and, particularly, gravity field solutions is investigated in this work. The main findings are that the first updates increasing the bandwidth from 0.25 Hz to 0.5 Hz help to significantly improve the quality of Swarm gravity fields and that the improvements are even larger than those achieved by GPS data rejection. It is also shown that these improvements are indeed due to an improved quality of GPS observa-

*Corresponding author
Email addresses: dahle@gfz-potsdam.de (C. Dahle), daniel.arnold@aiub.unibe.ch (D. Arnold), adrian.jaeggi@aiub.unibe.ch (A. Jäggi)

tions around the geomagnetic equator, and not due to missing observations in these regions. As the ionospheric activity is rather low in the most recent months, the effect of the tracking loop updates in summer 2016 cannot be properly assessed yet. Nevertheless, the quality of Swarm gravity field solutions has already improved after the first updates which is especially beneficial in view of filling the upcoming gap between the GRACE and GRACE Follow-on missions with hl-SST gravity products.

Keywords: Swarm; GPS high-low SST; Ionospheric scintillation; GPS Tracking loop; Gravity field; Geomagnetic equator

1. Introduction

The Swarm mission, launched in November 2013 by the European Space Agency (ESA) to primarily study the Earth's magnetic field (Friis-Christensen et al., 2008), consists of three identically built satellites each orbiting the Earth in a near-polar low Earth orbit (LEO). As the satellites are equipped with geodetic-quality Global Positioning System (GPS) receivers and star cameras, the Swarm mission also serves as candidate for Earth gravity field recovery by means of high-low satellite-to-satellite tracking (hl-SST). First results indicate that Swarm-derived gravity field solutions are generally of comparable quality w.r.t. corresponding hl-SST solutions derived from a dedicated gravity field mission such as the Gravity Recovery and Climate Experiment (GRACE) (Bezděk et al., 2016; Jäggi et al., 2016; Zehentner and Mayer-Gürr, 2016). However, there were also systematic deficiencies identified when processing GPS observations of the Swarm satellites. Swarm GPS observations are affected by ionospheric scintillation (Buchert et al., 2015; Sust et al., 2014), resulting in significantly larger carrier phase residuals of both reduced-dynamic and kinematic Swarm precise science orbits over the geomagnetic poles and around the geomagnetic equator (van den IJssel et al., 2015). It should be noted that kinematic orbits are more sensitive to errors in GPS observation data than reduced-dynamic orbits. Jäggi et al. (2016) confirmed this clear geographical dependency for the kinematic orbit solutions processed at AIUB and showed that in particular the problems around the geomagnetic equator are propagated into Swarm gravity field solutions when these kinematic orbit positions are used as pseudo-observations. The magnitude of these systematic errors varies depending on the ionospheric activity. Similar deficiencies were already observed for the GOCE mission by

Jäggi et al. (2015) who applied a data screening on the level of GPS observations in order to get rid of such systematic errors. The same kind of data screening has been adapted for Swarm by Jäggi et al. (2016) resulting in a significant decrease of the errors around the geomagnetic equator. However, by applying this method the errors did not fully vanish in all months on the one hand and additional long wavelength errors in the gravity field solutions could be introduced on the other.

In order to improve the quality and number of tracked GPS observations, several modifications regarding the GPS receiver settings onboard the Swarm satellites have been implemented during the mission. In particular, the tracking loop settings have been modified to achieve more robustness against ionospheric scintillation. A first analysis already showed a positive impact of the first tracking loop updates on the Swarm orbits (van den IJssel et al., 2016). In another study, focusing on the total loss of GPS signals, Xiong et al. (2016) also observed improvements after the first tracking loop update, but could only analyze a relatively short time span making it difficult to separate a possible positive influence of the modified tracking loop settings from improvements caused by less ionospheric activity during that period.

The focus of this work is on the influence of the tracking loop modifications on Swarm gravity field solutions. First, the impact of the ionosphere on GPS observations and precise LEO orbits derived thereof is recalled in Section 2. Section 3 gives an overview of the modifications that were applied to the Swarm GPS receivers, in particular of the different tracking loop settings and how their influence on Swarm gravity field solutions can be assessed. In Section 4, results are presented and discussed.

2. Impact of the ionosphere on GPS signals

The propagation of a microwave signal of frequency f transmitted by GPS satellites is dispersively affected by the free electrons in the Earth's ionosphere:

$$\Delta\rho_{ion} = \pm\frac{C_X}{2}Ef^{-2} + \mathcal{O}(f^{-3}) \tag{1}$$

where $\Delta\rho_{ion}$ is the path delay due to the ionosphere, $C_X/2 \approx 40\,\mathrm{m^3 s^{-2}}$ is a constant and $E = \int N_e(\rho)d\rho$ is the line-of-sight total electron content (TEC), obtained by integrating the electron density N_e along the ray path. The negative sign in Eq. (1) refers to the phase advance of the carrier phase

observations, the positive sign to the group delay of the code observations, respectively. As GPS satellites transmit microwave signals at two frequencies ($f_1 = 1575.42\,\mathrm{MHz}$ and $f_2 = 1227.60\,\mathrm{MHz}$), an ionosphere-free linear combination $L_{if} = (f_1^2 L_1 - f_2^2 L_2)/(f_1^2 - f_2^2)$ of the two original carrier phase observations L_1 and L_2 can be used in order to eliminate the ionospheric refraction proportional to f^{-2}. The terms $\mathcal{O}(f^{-3})$ are called higher-order ionospheric (HOI) corrections. They are not eliminated by forming L_{if}. Their modeling requires the knowledge of the electron density and the magnetic field along the ray path (Hoque and Jakowski, 2008). All orbit and gravity field solutions presented in this work are obtained by using only L_{if}. In Jäggi et al. (2015) some attempts were made to mitigate ionosphere-induced problems in precise orbit determination (POD) of the GOCE satellite by means of HOI modeling, but the success was marginal. Thus, no HOI corrections are taken into account in this work. As another error source, irregularities in the spatial distribution of N_e can cause temporal fluctuations in intensity and phase of the received GPS signal. This effect is known as ionospheric scintillation and is not necessarily eliminated by L_{if} (van den IJssel et al., 2016). It mainly occurs around the equator, where both intensity and phase fluctuations are present, and in polar regions, where rather phase fluctuations are the dominant type of scintillation. In equatorial regions, more precisely along two bands north and south of the geomagnetic equator, ionospheric scintillation mostly occurs after local sunset (Basu et al., 2002). Furthermore, its occurence and intensity also depends on geomagnetic activity and has a seasonal component as well. Fig. 1 (left) shows Swarm-A carrier phase residuals of two days with comparable orbit-Sun geometry (day 2015/111: local time of ascending arc $\sim 17\,\mathrm{h}$, day 2015/233: local time of descending arc $\sim 18\,\mathrm{h}$), but with substantially different mean TEC in the Earth's ionosphere, see Fig. 1 (right). It can be seen that residuals are largest near the poles and also large in equatorial regions, and they are systematically smaller on day 2015/233, when the ionospheric activity is relatively low. This strongly suggests that systematic deficiencies in Swarm precise science orbits (van den IJssel et al., 2015; Jäggi et al., 2016) and gravity field solutions (Jäggi et al., 2016) are caused by ionospheric scintillation.

The dynamics of the ionosphere can be directly derived from the GPS data by forming the so-called geometry-free linear combination $L_{gf} = L_1 - L_2$, which, up to a carrier phase ambiguity, corresponds to the ionospheric refraction. A closer look into polar and equatorial regions reveals that the nature of corresponding ionospheric disturbances occuring there is differ-

ent. This can be seen by analyzing the time derivative of the geometry-free linear-combination dL_{gf}/dt characterizing the rate of change of ionospheric refraction. Fig. 2 (left) shows dL_{gf}/dt computed from the observations of the Swarm-A receiver to one GPS satellite (PRN05) during 15.6 minutes of a polar pass (from latitudes $-60.0°$ to $-87.4°$ back to $-60.0°$). From minute 1304 ($\phi = -76.2°$) onwards the ionospheric refraction shows massive high-frequency variations, most probably caused by scintillation, resulting in a higher noise also in the L_{if} phase residuals. Such passes are very common for GPS observations gathered by spaceborne receivers at high latitudes and have been observed e.g. for the GOCE mission (Bock et al., 2014; Jäggi et al., 2015). Fig. 2 (right) shows the daily RMS values of dL_{gf}/dt for all Swarm satellites for polar passes. Note the clear correlation with the daily mean TEC in Fig. 1 (right). In Fig. 3 (right), the highpass-filtered part of the geographically binned RMS of dL_{gf}/dt over the months November and December 2014 is plotted showing that such high-frequency variations are mainly present in polar regions. In equatorial regions, these scintillation-like features are much less pronounced and the more important phenomena are slower variations of dL_{gf}/dt with larger amplitudes. In contrast to polar areas, the variations of dL_{gf}/dt do not coincide with a notably increased noise in the L_{if} phase residuals here. This is illustrated in Fig. 4 (left) showing an equatorial pass (from $30.0°$ to $-30.0°$) for Swarm-A. Around latitudes $\phi = 8°$ and $\phi = -18°$ the difference between a reduced-dynamic and the kinematic orbit shows short deviations of several centimeters. Due to the stiffness of the reduced-dynamic orbit (6 minutes piecewise constant empirical accelerations were set up), these deviations have to be attributed to the kinematic orbit and will be subsequently mapped into a gravity field solution recovered from these kinematic positions. However, when using orbit positions as pseudo-observations for gravity field recovery, it is advisable to use a kinematic rather than a reduced-dynamic orbit as the latter inherently contains a priori information of the gravity field and other dynamic forces that tends to bias the estimated solution. Daily RMS values of dL_{gf}/dt for all Swarm satellites for equatorial passes are shown in Fig. 4 (right). The values of the full signal are larger compared to those for polar passes shown in Fig. 2 (right) which is also confirmed by Fig. 3 (left) in the spatial domain.

A rather crude, but proven method for the mitigation of ionosphere-induced problems of orbits and gravity fields is the simple omission of GPS observations with dL_{gf}/dt exceeding a certain threshold (see Jäggi et al. (2016) for more details). While for GOCE, a suitable threshold was found to

be 5 cm/s (Jäggi et al., 2015), a more stringent value of 2 cm/s had to be applied for Swarm (Jäggi et al., 2016) indicating that the GPS receivers onboard Swarm were initially more sensitive to ionospheric disturbances than the one onboard GOCE. Depending on seasonal variations in the mean TEC, this can lead to approx. 10 % of maximum discarded Swarm GPS observations per day. Although the systematic features around the geomagnetic equator are significantly reduced in the resulting gravity field solutions, they do not fully disappear in periods with high ionospheric activity. Further drawbacks are slightly larger residuals of independent orbit validation by means of Satellite Laser Ranging (SLR) and a degradation of the very low degrees of certain gravity field solutions. This is most probably caused by a number of weakly determined kinematic orbit positions due to too many missing observations after the data screening.

Generally, the effect of ionospheric scintillation on space-borne GPS observations also depends on the specific architecture of a GPS receiver (van den IJssel et al., 2016). For instance, hl-SST orbits and gravity fields derived from GPS observations of the GRACE mission are not, or at least very much reduced, affected by ionosphere-induced features (Jäggi et al., 2016). By analyzing the number of missing GPS observations (i.e. a GPS satellite has not been observed on both frequencies at a particular epoch) during March 2014, it becomes clear that the Swarm and GRACE GPS receivers behave differently under similar ionospheric conditions (see Jäggi et al., 2016, Fig. 14). During that period, the ascending arcs of GRACE and the descending arcs of Swarm-A passed the equator in the evening hours and the TEC was relatively high (38 to 44 TECU). While the Swarm-A receiver shows almost no missing observations, the GRACE-B receiver skips a significant number of observations along the geomagnetic equator. Assuming that these missing observations are correlated with ionospheric disturbances, this explains why spurious signals along the geomagnetic equator are not propagated from kinematic orbits into gravity field solutions in case of GRACE.

3. Swarm GPS receiver modifications

During the Swarm mission, the settings of the three satellites' GPS receivers have been modified several times in order to improve the GPS tracking performance. All modifications and their dates (up to autumn 2016) are summarized in Table 1 from which it becomes obvious that two different kind of modifications have been commanded: 1) changes in the antenna field of

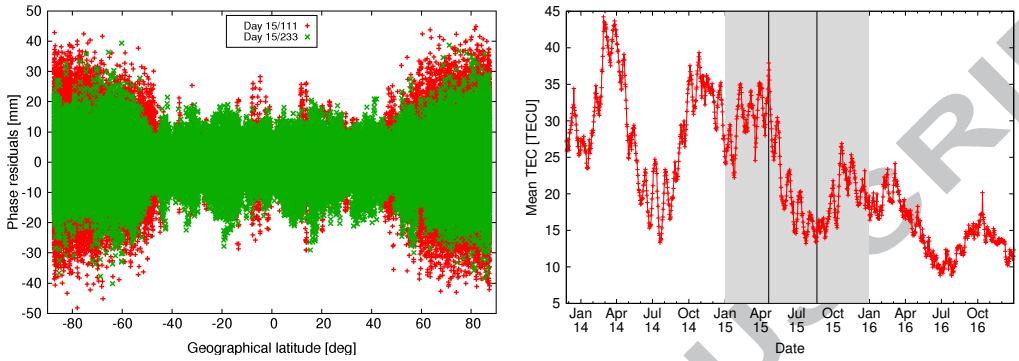

Figure 1: Left: carrier phase residuals of kinematic Swarm-A POD for days 2015/111 (April 21st, 2015) and 2015/233 (August 21st, 2015). Right: daily mean TEC as derived by the Center for Orbit Determination in Europe (CODE). The two vertical lines mark the days 2015/111 and 2015/233, the period with grey background matches the period shown in Fig. 2 (right). 1 TECU $\equiv 10^{16}$ electrons/m^2.

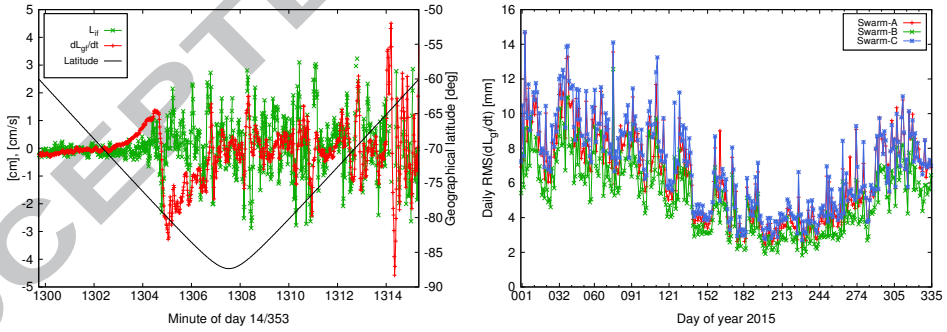

Figure 2: Left: dL_{gf}/dt (red), L_{if} carrier phase residuals of kinematic POD (green) and geographical latitude (black) for Swarm-A passing the south pole on day 2014/353 (December 19th, 2014). Right: daily RMS of dL_{gf}/dt over all GPS satellites for polar passes ($|\phi| > 60°$) in the year 2015.

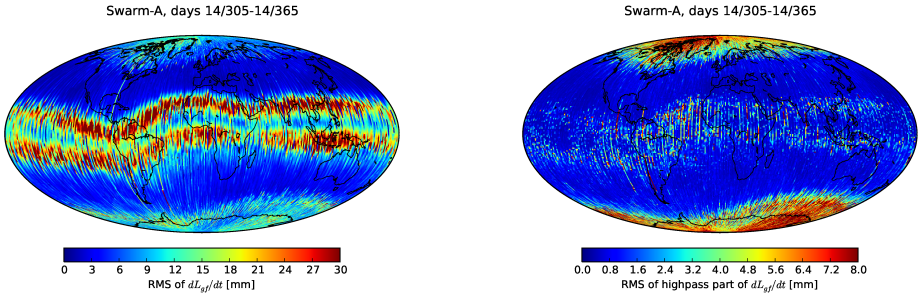

Figure 3: Geographically binned RMS of dL_{gf}/dt for Swarm-A. Left: full signal. Right: highpass-filtered signal (a Gauss filter of width 100 s was used to filter each pass).

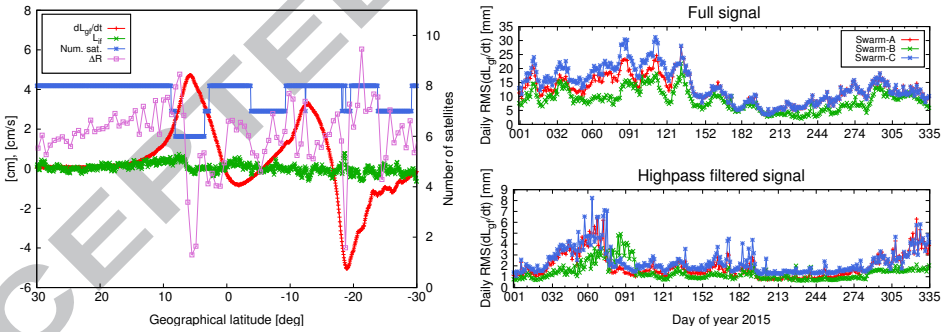

Figure 4: Left: dL_{gf}/dt (red), L_{if} carrier phase residuals of kinematic POD (green), number of GPS satellites used for kinematic positioning (blue) and difference in radial direction between reduced-dynamic and kinematic orbit (magenta) for Swarm-A passing the equator on day 2014/305 (November 1st, 2014) west of South America. Right: daily RMS of dL_{gf}/dt over all GPS satellites for equatorial passes ($|\phi| < 30°$) in the year 2015 (top: full signal, bottom: highpass-filtered signal).

view (FoV), i.e. a reduction of the elevation mask, and 2) changes in the receiver tracking loop settings.

The former had the intention to increase the number of simultaneously tracked GPS satellites. As each of the Swarm GPS receivers has only eight channels, this number is already limited compared to other LEO satellites, and in connection with the originally implemented FoV of 80°, the maximum number of eight GPS satellites tracked was reached only during 50 % of the time (van den IJssel et al., 2016). The antenna FoV modifications are not directly related to the aforementioned problems caused by ionospheric disturbances and thus are not investigated in this work. However, it should be noted that the empirical GPS antenna phase center variations (PCVs) for Swarm as described in Jäggi et al. (2016) needed to be recomputed in order to achieve highest possible accuracy also for the most recent periods with an enlarged antenna FoV.

The focus in this work is on the latter kind of modification, i.e. changes in the tracking loop settings, as these were primarily intended to improve the robustness of GPS tracking in difficult environmental situations caused by ionospheric scintillation[1]. Generally, a GPS receiver's bandwidth should be wide enough to accommodate not only usual changes in Doppler shift of the phase signals, but also phase fluctuations during periods of intense amplitude and phase scintillation. If this is not the case, an increase in the loss of GPS data and cycle slips due to effects of ionospheric scintillation could be expected.

Table 1 also shows that the modifications were done stepwise and not simultaneously for all three satellites. Regarding the tracking loop settings, the original bandwidth was set to 0.25 Hz and has been widened in steps of 0.25 Hz. Currently (in autumn 2016), the largest bandwidth is 1 Hz for Swarm-C. Updates were always implemented first on Swarm-C and then after a few weeks or even months passed, the same updates were also applied for Swarm-A and (so far only in case of the first update) also for Swarm-B. Thus, there are certain periods where Swarm-A and -C have different tracking loop settings, but identical GPS receiver settings apart from that. As these two Swarm satellites fly around the Earth close-by to each other in virtually the same orbits, a comparison of their individual results should reflect a possible

[1] https://earth.esa.int/web/guest/missions/esa-operational-eo-missions/swarm/news/-/asset_publisher/K3vp2LwLXSrF/content/swarm-gpsr-update-may-2015

Table 1: Overview of Swarm GPS receiver modifications.

Date	Satellite	Modification			
2014/10/21	Swarm-A	Antenna FoV:	80°	→	83°
2014/10/22	Swarm-B	Antenna FoV:	80°	→	83°
	Swarm-C	Antenna FoV:	80°	→	83°
2014/12/01	Swarm-C	Antenna FoV:	83°	→	86°
2015/01/13	Swarm-C	Antenna FoV:	86°	→	88°
2015/05/06	Swarm-A	Antenna FoV:	83°	→	88°
	Swarm-B	Antenna FoV:	83°	→	88°
	Swarm-C	L_1 TL[a] bandwidth:	10 Hz	→	15 Hz
		L_2 TL bandwidth:	0.25 Hz	→	0.5 Hz
2015/10/08	Swarm-A	L_1 TL bandwidth:	10 Hz	→	15 Hz
		L_2 TL bandwidth:	0.25 Hz	→	0.5 Hz
2015/10/10	Swarm-B	L_1 TL bandwidth:	10 Hz	→	15 Hz
		L_2 TL bandwidth:	0.25 Hz	→	0.5 Hz
2016/06/23	Swarm-C	L_2 TL bandwidth:	0.5 Hz	→	0.75 Hz
2016/08/11	Swarm-A	L_2 TL bandwidth:	0.5 Hz	→	0.75 Hz
	Swarm-C	L_2 TL bandwidth:	0.75 Hz	→	1 Hz

[a] tracking loop

influence of the tracking loop updates. This is done in the next section.

4. Results

The Swarm gravity field solutions presented in this section are computed using the Celestial Mechanics Approach (Beutler et al., 2010) following the method by Jäggi et al. (2011a). Kinematic Swarm orbits, required as pseudo-observations, have been computed at AIUB using the same processing strategy as described in Jäggi et al. (2016) execpt for the updated antenna PCVs mentioned in Section 3. Two versions of kinematic orbits have been generated: For the first, all available GPS observations as provided by ESA in the official Level-1 product have been used (labelled as "original" in the following), whereas for the second version, an additional data screening as mentioned in Section 2 has been applied before the POD (labelled as "screened" in the following). Consequently, also two versions of gravity field solutions

have been generated, based on either of the two orbit versions. The processing details regarding gravity field determination are the same as outlined in Jäggi et al. (2016) except for the following differences: The static part of the AIUB-GRACE03S model (Jäggi et al., 2011b) is now used up to degree and order 90 as a priori background model for the gravity field, EOT11a (Savcenko and Bosch, 2012) is now used as ocean tide background model, and additional background models for non-tidal short-term variations in atmosphere and oceans (AOD1B; Dobslaw et al., 2013) and ocean pole tide (model by Desai; Petit and Luzum, 2010) have been added.

In Fig. 5, the standard deviation of the carrier phase residuals of the kinematic POD ("original" orbits) for Swarm-A, -B and -C is plotted giving an impression of the quality of kinematic positions. It can be seen that after the three satellites were placed in their dedicated orbits (around end of March 2014), Swarm-B flying at a higher altitude has a systematically smaller standard deviation whereas Swarm-A and -C show more or less the same values when looking at monthly averages. This situation suddenly changes in May 2015, i.e. right after the first tracking loop update from 0.25 Hz to 0.5 Hz only on Swarm-C, and the standard deviations are now significantly smaller for this satellite compared to the co-orbiting Swarm-A and even smaller than for Swarm-B. After October 2015, when the tracking loop settings on Swarm-A and -B were also updated to the same bandwidth again as for Swarm-C, the same situation as before the first updates can be observed. The further tracking loop changes on Swarm-C and -A in June and August 2016, respectively, do not cause likewise detectable features. In a more detailed analysis, the carrier phase residuals are analyzed separately in polar and equatorial regions. Fig. 6 shows that the first tracking loop changes mainly decrease the carrier phase residuals at high latitudes (compare Swarm-A and -C between days 126 and 281). Around the equator, there is no visible effect that can be apparently related to tracking loop updates. This is unsurprising though, since ionosphere-induced systematic effects in these regions do not necessarily come along with larger carrier phase residuals, as already mentioned earlier in Section 2, Fig. 4 (left).

However, the updated tracking loop settings are also able to substantially reduce the artifacts along the geomagnetic equator as can be seen by looking at monthly gravity field solutions for June 2015 (the first complete month with updated settings on Swarm-C and the original settings on Swarm-A and -B). This is illustrated in Fig. 7 showing geoid height maps of individual monthly Swarm-A and -C solutions both for the "original" and "screened"

case. The geoid variations are relative to the GOCO05s model (Mayer-Gürr et al., 2015), the time-variable linear trends of which have been evaluated at the epoch 2014/09/01, and Gaussian smoothing with 400 km radius is applied. Looking at the "original" solutions, one can see a more pronounced pattern of the geomagnetic equator for Swarm-A. The "screened" solutions are better than the "original" ones for both Swarm-A and -C. Yet it has to be noted that the "screened" Swarm-A solution is still worse than the "original" Swarm-C solution which is reflected by the unlikely physically meaningful geoid anomalies in the Sahara as well as a larger global weighted root mean square (wRMS) value. It has to be mentioned that this obvious improvement due to the tracking loop update on Swarm-C is not related to an increased number of missing GPS observations as already reported for GRACE in Section 2. The number and spatial distribution of missing observations in June 2015 for Swarm-A and -C is shown in Fig. 8. As no systematic differences are visible, the conclusion is that the GPS data collected in equatorial regions is corrupted prior to the first tracking loop update. One might of course argue that 400 km Gaussian smoothing is too optimistic for monthly Swarm gravity field solutions and the shown effects are smaller than the overall noise level, but the same conclusions can still be drawn even when a relatively strong Gaussian smoothing with 750 km radius is applied (Fig. 9). The latter roughly corresponds to the spatial resolution of 1666 km up to which monthly Swarm solutions are able to describe time-variable gravity signals comparable to monthly GRACE K-Band solutions (Encarnação et al., 2016). Note that the C_{20} coefficient (describing the Earth's flattening) of the solutions shown in Fig. 9 has been replaced by the SLR-derived value provided in GRACE Technical Note 07 (Cheng and Ries, 2016) as the error of this coefficient would otherwise dominate the geoid plots.

Table 2 lists the global wRMS values after 400 km Gaussian smoothing of the individual "original" and "screened" solutions for Swarm-A and -C as well as quantities derived thereof and the averaged mean TEC over one month as indicator for the ionospheric activity for the 17 months from March 2015 till July 2016. First of all, a clear correlation between the size of the mean TEC and the size of the wRMS, in particular of the "original" solutions, can be seen. Furthermore, the data screening effectively helps to improve those gravity field solutions where the initial tracking loop bandwidth of 0.25 Hz is active and the mean TEC is relatively high at the same time. This is illustrated by the values for the relative change of the "screened" solutions w.r.t. to the corresponding "original" solution which show clear improvements of

double-digit %-numbers for both Swarm-A and -C during the period March till May 2015 when the mean TEC is 24 TECU or higher. In the period June till September 2015, the mean TEC decreased below 20 TECU and additionally, the tracking loop settings are different now for Swarm-A and -C. For Swarm-A with the initial bandwidth, the data screening yields still improvements of 6 to 13 %, whereas for Swarm-C with a wider bandwidth of 0.5 Hz, the wRMS values of the "original" and "screened" solutions become much closer to each other and the "screened" solution is not always the better one. This more or less random behavior of the relative change due to the data screening is also the case for all solutions after September 2015 for both satellites. As a conclusion, it can be stated that the effect of GPS data screening has become much less significant after the first tracking loop update, i.e. the quality of Swarm gravity field solutions does not depend as strongly as before on using either "original" or "screened" kinematic orbits. However, this statement might not be valid anymore in case the ionospheric activity increases again in the future e.g. when the satellites' altitude has become lower. Another indication for the positive impact of the first tracking loop update on gravity field recovery is the agreement between the individual single-satellite solutions in one particular month. As such a measure, Table 2 shows the absolute differences between the wRMS values of the best (i.e. either "original" or "screened") Swarm-A and -C solution. In months with identical tracking loop settings on both satellites, this minimum absolute difference is 2.1 mm and 0.7 mm in March and April 2015, respectively, when the mean TEC is high and the solutions are generally worse, but is remarkably low (not larger than 0.5 mm) in the period November 2015 till May 2016. For the months June till September 2015 with different tracking loop settings, the minimum absolute difference has its overall maximumn value of more than 5 mm in June 2015 and is approx. 1 mm in the other three months, although the mean TEC is comparable to the period November 2015 till May 2016. During these four months, it is always a Swarm-C solution showing the smallest wRMS and thus the "original" Swarm-C solution performs always better than the "screened" Swarm-A solution which clearly supports the conclusion that Swarm gravity fields benefit from the updated tracking loop bandwidth of 0.5 Hz. As before, no influence of the tracking loop update on Swarm-C in June 2016 is visible, but the mean TEC during this month is extremely low with approx. 10 TECU. Closing the discussion of Table 2, it has to be mentionend that most findings could also be derived from the wRMS values of the more appropriately smoothed solutions with 750 km Gaussian

filter radius (not shown). Yet, due to the much stronger smoothing of the solutions, e.g. the differences between the values for the minimum absolute differences become less pronounced and the different behavior of Swarm-A and -C in the period July till September 2015 as described above cannot be detected anymore.

A similar picture can be drawn by analyzing the gravity field solutions in the spectral domain, i.e. by means of difference degree amplitudes w.r.t. a state-of-the-art static gravity field model (again, GOCO05s is used here). As long as the original tracking loop settings have been active, Swarm-A and -C "original" solutions look very similar. When the data screening is applied, the difference degree amplitudes for both satellites become significantly smaller already for relatively low degrees (approx. around degree $n = 15$). Since smaller differences w.r.t. to a much more accurate reference model indicate a better signal-to-noise ratio of the solution to be compared, this is another confirmation that improvements can be obtained by the data screening. A typical example for this case is March 2015 shown in Fig. 10 (top left). In the period between the first update on Swarm-C until the first update on Swarm-A, Swarm-C solutions always perform better. Furthermore, during this whole period, the effect of modified tracking loop settings exceeds the effect of the GPS data screening, at least with the applied screening criterion of $dL_{gf}/dt > 2\,\mathrm{cm/s}$. In June 2015 (Fig. 10, top middle), the data screening has rather little impact on the solutions for both Swarm-A and -C whereas, e.g., in September 2015 (Fig. 10, top right), this is only true for Swarm-C with the increased tracking loop bandwidth. For Swarm-A with the original bandwidth, the data screening improves the solution, but still does not reach the "original" Swarm-C solution. After October 2015, when also Swarm-A has an increased bandwidth, Swarm-A and -C solutions perform always similar to a very large extent. As already the case for Swarm-C since June 2015, the data screening does not have any significant influence on the degree amplitudes. Representing this period, Fig. 10 (bottom left) shows the solutions for March 2016. In order to investigate a possible influence of the tracking loop updates on 2016/06/23 and 2016/08/11, solutions for the periods 2016/06/24 till 2016/08/10 (Fig. 10, bottom middle) and 2016/08/12 till 2016/09/10 (Fig. 10, bottom right) have been generated. During these periods, Swarm-A and -C have different tracking loop settings again, but this further increase of the bandwidths does not affect the gravity field solutions.

Based on the results presented so far in this section, it can be concluded that the effect of widening the tracking loop bandwidth from originally

0.25 Hz to 0.5 Hz is clearly detectable and generally beneficial for Swarm gravity field recovery. This is also indicated by the time series of monthly equivalent water height (EWH) averages for the Amazon basin which is an example for a typical scientific application of monthly Swarm gravity field solutions, in particular in absence of the GRACE mission or its successor GRACE Follow-on (GRACE-FO, Flechtner et al. (2016)). Fig. 11 shows the comparison between one of the dedicated GRACE K-Band solutions, GFZ RL05a (Dahle et al., 2012), and the combined solution from Swarm-A, -B and -C processed at AIUB. It can be seen that the Swarm time series generally matches quite well with GRACE, but looks noisier during the first part of the mission. Yet, improvements are clearly visible in recent months where the fit between Swarm and GRACE looks remarkably well now. These improvements start in mid of 2015 exactly coinciding with the first tracking loop update. However, the ionospheric activity has decreased as well in the same period (Fig. 1, right) which could also be the reason for obtaining better results. Thus, a more meaningful conclusion about the influence of the tracking loop settings could only be made by analyzing longer time series hoping that periods with different tracking loop bandwidths, but comparable ionospheric properties and orbit geometry are available. The relatively low ionospheric activity in recent months could also explain why the tracking loop updates to 0.75 Hz and 1 Hz are not visible so far. Further analysis of results in the upcoming ionosphere season with increased activity is required to draw a final conclusion for this question.

5. Summary

GPS-based LEO POD and subsequent hl-SST gravity field recovery can be significantly affected by ionospheric disturbances, even when using the ionosphere-free linear combination L_{if}. Here, orbits and gravity field solutions based on GPS data of the Swarm mission are investigated. Particularly in the first approx. 18 months of the mission, kinematic orbits of the Swarm satellites show deficiencies in both polar regions and around the geomagnetic equator. By analyzing the first time derivative of the geometry-free linear combination L_{gf}, it is shown that different mechanisms act in these two regions. At high latitudes, mainly high-frequency scintillation-like features occur resulting in larger carrier phase residuals. Equatorial crossings are rather characterized by large, but deterministic changes of dL_{gf}/dt which are not reflected by larger residuals, but cause systematic biases in the kine-

Table 2: Global wRMS values of monthly geoid variations [mm] (after 400 km Gaussian smoothing) w.r.t. GOCO05s for Swarm-A and -C "original" ($\mathrm{wRMS}^{A/C}_{ori}$) and "screened" ($\mathrm{wRMS}^{A/C}_{scr}$) solutions and their relative change (RC)[a] in %, the minimum absolute differences ($|\Delta|_{min}$)[b] between Swarm-A and -C wRMS values and the daily mean TEC values [TECU] shown in Fig. 1 (right) averaged over one month.

Month	Swarm-A wRMS^{A}_{ori}	wRMS^{A}_{scr}	RC^{A}	Swarm-C wRMS^{C}_{ori}	wRMS^{C}_{scr}	RC^{C}	$\lvert\Delta\rvert_{min}$	average mean TEC	identical TL settings
2015/03	27.3	15.6	-42.9	28.2	13.5	-52.1	2.1	31.5	yes
2015/04	25.3	14.4	-43.1	28.2	15.1	-46.5	0.7	32.1	yes
2015/05	20.8	13.5	-35.1	15.8	11.5	-27.2	2.0	24.5	partly[c]
2015/06	15.7	14.7	-6.4	10.1	9.5	-5.9	5.2	19.0	no
2015/07	10.7	10.0	-6.5	9.0	9.0	0	1.0	16.7	no
2015/08	11.4	10.4	-8.8	9.5	9.7	2.1	0.9	15.5	no
2015/09	14.8	12.8	-13.5	11.4	11.9	4.3	1.4	16.9	no
2015/10	13.2	13.0	-1.5	12.3	12.6	2.4	0.7	21.2	partly[c]
2015/11	11.2	10.7	-4.5	11.3	11.1	-1.8	0.4	22.5	yes
2015/12	10.7	11.1	3.7	10.7	11.2	4.7	0	19.6	yes
2016/01	10.5	10.7	1.9	10.5	10.5	0	0	17.9	yes
2016/02	12.8	14.4	12.5	13.0	14.1	8.5	0.2	20.2	yes
2016/03	11.2	11.5	2.7	11.2	11.1	-0.9	0.1	19.8	yes
2016/04	9.2	9.3	1.1	8.8	8.9	1.1	0.4	16.2	yes
2016/05	8.6	8.7	1.2	8.1	8.3	2.5	0.5	14.0	yes
2016/06	8.4	8.6	2.4	8.5	8.5	0	0.1	10.7	partly[c]
2016/07	7.5	7.5	0	7.5	7.6	1.3	0	10.4	no

[a] $\mathrm{RC}^{A/C} = (\mathrm{wRMS}^{A/C}_{scr} - \mathrm{wRMS}^{A/C}_{ori})/\mathrm{wRMS}^{A/C}_{ori}$
[b] $|\Delta|_{min} = |min(\mathrm{wRMS}^{A}_{ori}, \mathrm{wRMS}^{A}_{scr}) - min(\mathrm{wRMS}^{C}_{ori}, \mathrm{wRMS}^{C}_{scr})|$
[c] see Table 1

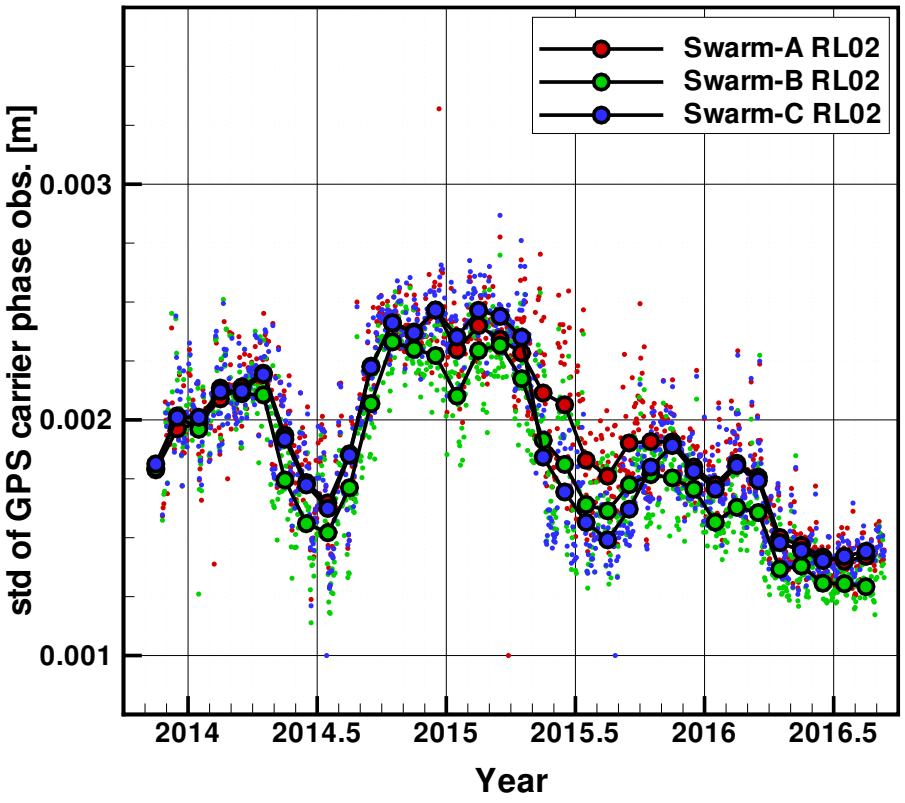

Figure 5: Standard deviation of carrier phase residuals of kinematic POD ("original" orbits) of SWARM-A, -B and -C. Small dots represent daily values, larger circles are monthly averages of the daily values.

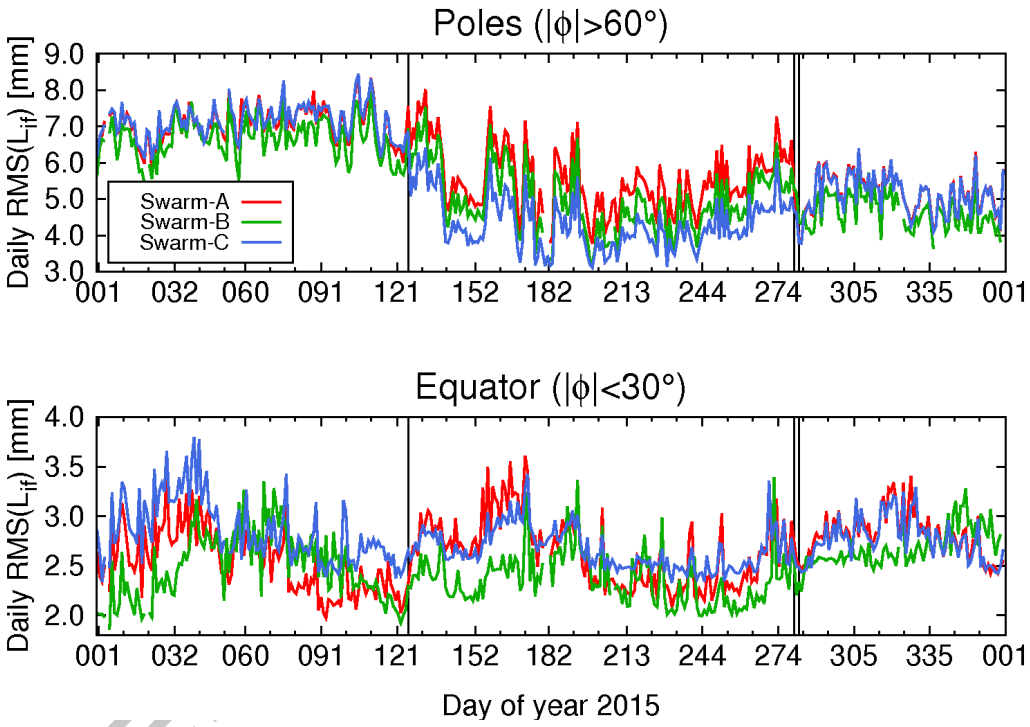

Figure 6: Daily RMS values of L_{if} carrier phase residuals of kinematic POD for polar (top) and equatorial (bottom) passes. The three vertical lines indicate the days on which the tracking loop updates occurred.

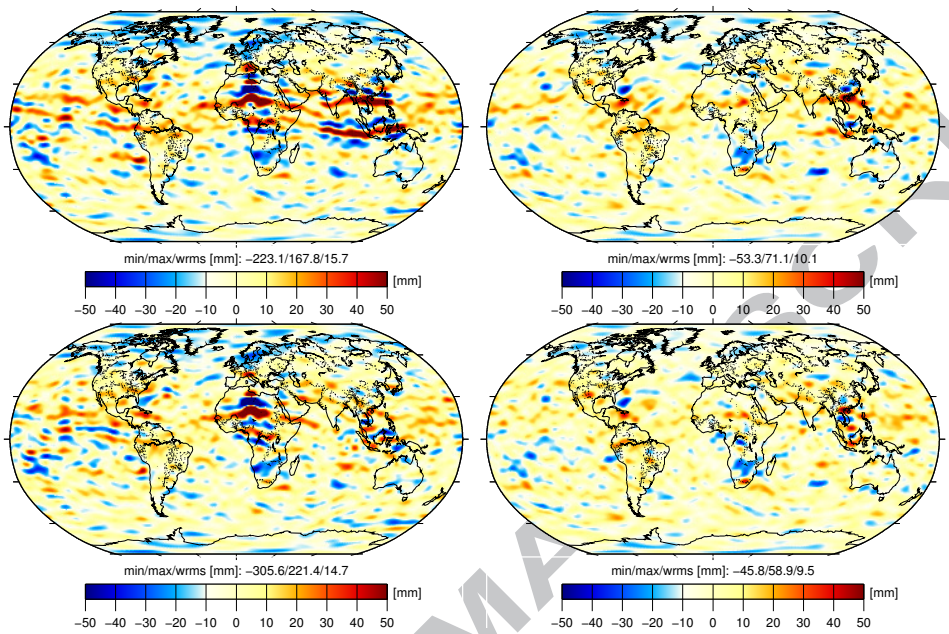

Figure 7: Geoid height variations w.r.t. GOCO05s of Swarm-A (left) and Swarm-C (right) individual monthly gravity field solutions for June 2015 based on "original" (top) and "screened" (bottom) kinematic orbits. Gaussian smoothing with 400 km radius is applied.

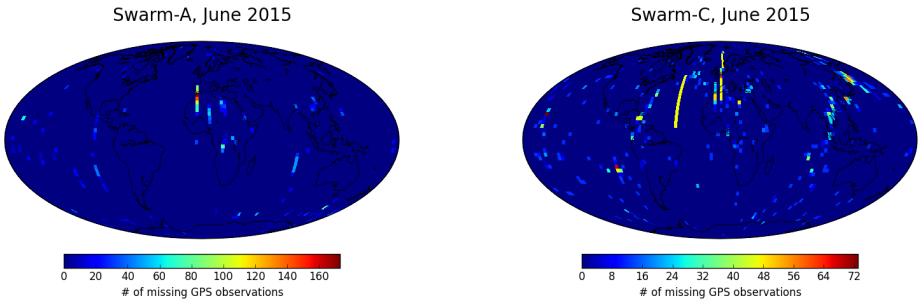

Figure 8: Number of missing GPS observations for Swarm-A (left) and Swarm-C (right) in June 2015.

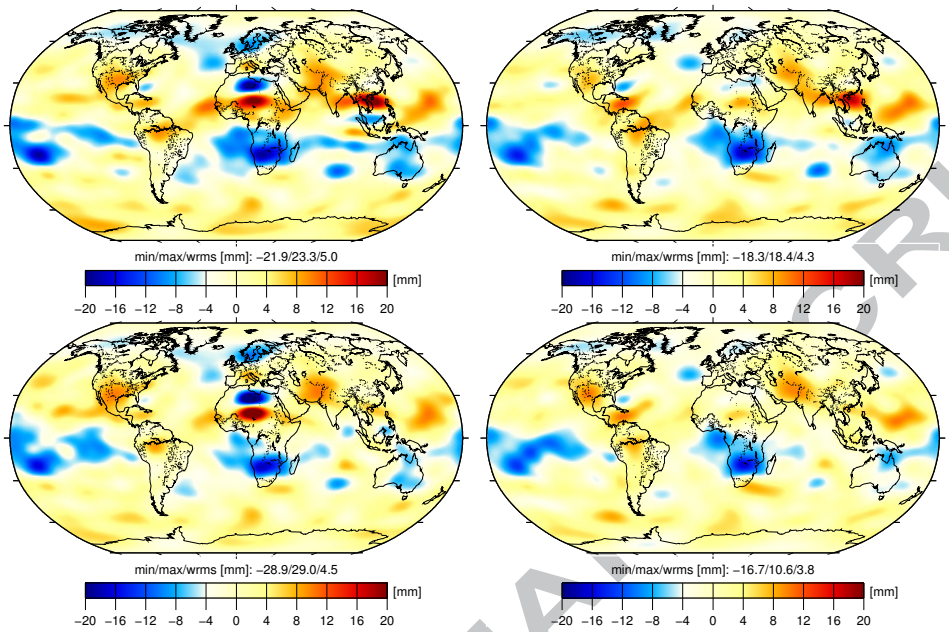

Figure 9: Same as Fig. 7, but with Gaussian smoothing with 750 km radius and C_{20} replaced.

matic orbit positions. The latter are mapped into gravity fields recovered from these kinematic orbits, whereas no degradation of gravity field solutions around the poles becomes visible. One possible explanation for these different mechanisms could be the distinction between diffractive and refractive scintillation; in equatorial regions the former kind is predominantly whereas in polar regions it is rather the latter kind (Sust et al., 2014). A thorough investigation would have exceeded the scope of this manuscript and further research is required to better understand this and other remaining questions like how are GPS phase measurements affected by different types of ionospheric disturbances and how can the related systematic errors be removed by adjusting receiver settings such as the tracking loop bandwidth.

In a first, data-driven attempt to mitigate these ionosphere-induced problems, the GPS observations are screened by simply omitting any observation where dL_{gf}/dt exceeds a threshold of 2 cm/s. Results based on this "screened" data show less pronounced systematic artefacts around the geomagnetic equator, but some systematic errors can still remain in the gravity solutions and the effectiveness of the data screening also depends on the

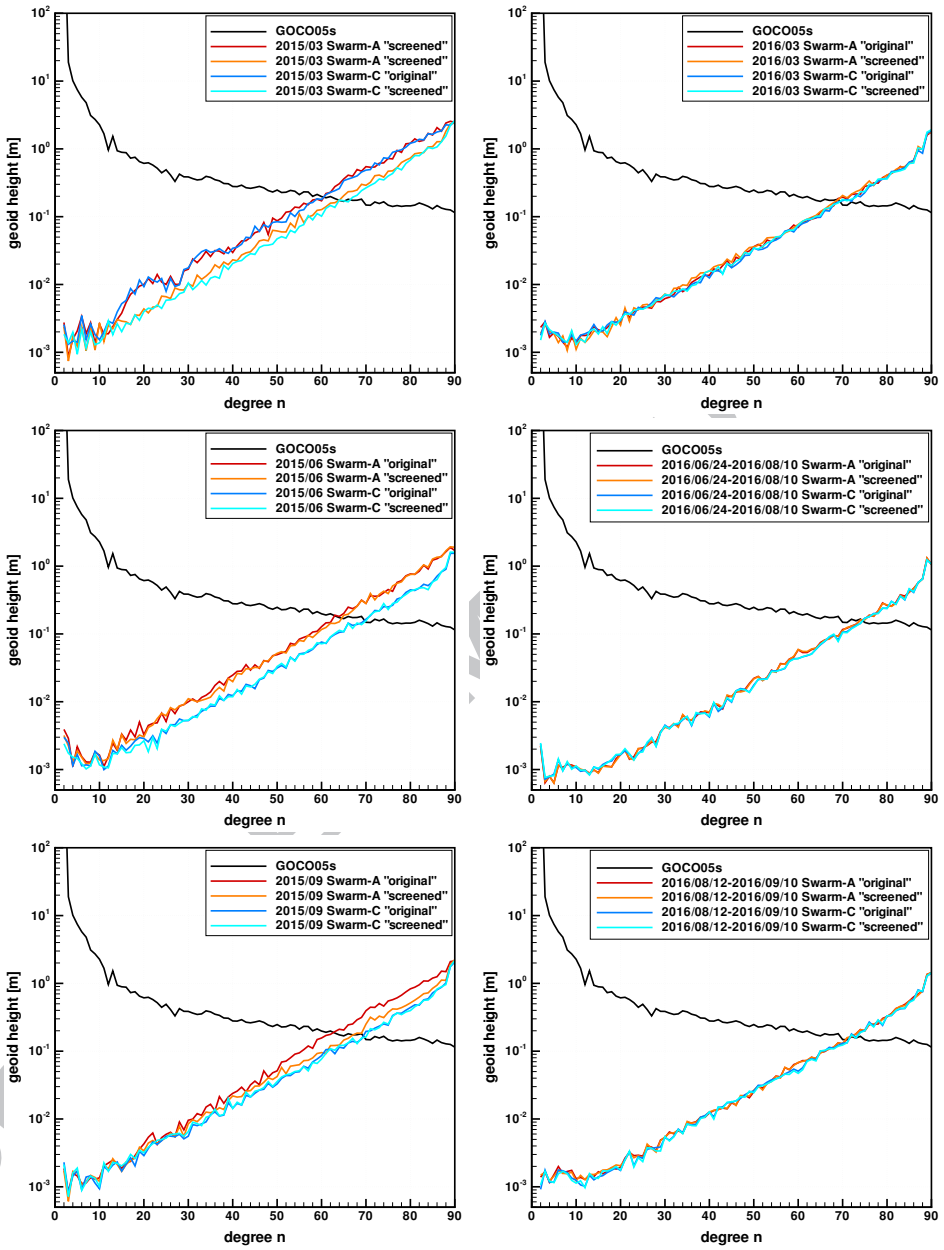

Figure 10: Degree amplitudes (in geoid height [m]) w.r.t. GOCO05s of Swarm-A/-C "original"/"screened" individual monthly gravity field solutions for March 2015 (top left), June 2015 (middle left), September 2015 (bottom left), March 2016 (top right), June/July/August 2016 (middle right) and August/September 2016 (bottom right).

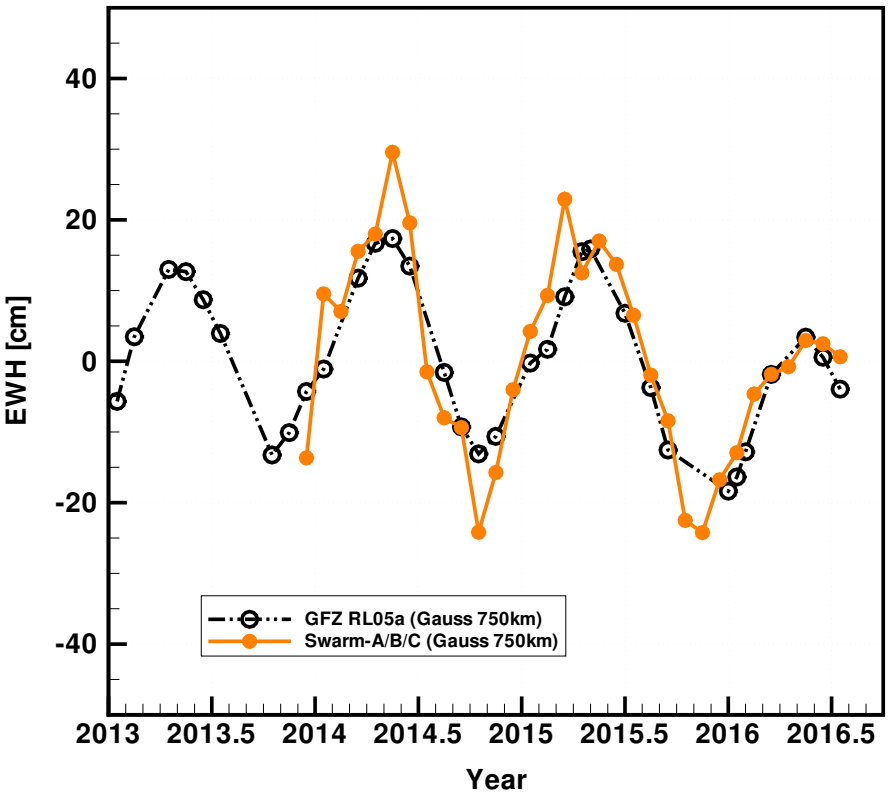

Figure 11: Basin average time series for the Amazon basin in terms of EWH [cm] for combined Swarm-A, -B, -C solutions based on "screened" GPS data and the GFZ RL05a GRACE solutions (Gaussian smoothing with 750 km radius is applied and C_{20} is replaced for both time series). Note that some months are missing in the GRACE time series.

ionospheric activity. Additionally, further drawbacks of this method are: "screened" orbits perform slightly worse in SLR orbit validation and the very low degrees of the gravity solutions, which are on the other hand the ones of most interest, can be degraded as well.

Since receiver-specific tracking problems were considered to be the main cause of the degradations, the GPS tracking loop bandwidths onboard Swarm have been increased stepwise starting in May 2015 on Swarm-C. By comparing gravity field results from the co-orbiting Swarm-A and -C satellites when both spacecrafts have different tracking loop settings, it becomes obvious that the first tracking loop update from 0.25 Hz to 0.5 Hz for L_2 helps to substantially improve Swarm gravity field solutions. This can be seen in the spatial domain, where the traces of the geomagnetic equator in the gravity field solutions are reduced, as well as in the spectral domain, where the difference degree amplitudes w.r.t. a static gravity field model decrease. These improvements are not related to missing GPS observations around the geomagnetic equator leading to the conclusion that parts of the Swarm GPS data gathered over this region are indeed corrupted as long as the tracking loop bandwidths are set to their original values. It can be concluded as well that the effect of the tracking loop settings exceeds the effect of the GPS data screening. The tracking loop bandwidth increase to 0.5 Hz also results in smaller L_{if} residual noise at high latitudes. This might be in particular beneficial for space baselines determined for orbit and gravity field computations. The further tracking loop updates to bandwidths > 0.5 Hz do not show any additional improvements so far. However, since the times they were implemented, the ionospheric activity has been relatively low and a possible impact on Swarm precise science orbits and gravity field solutions needs to be investigated as soon as a long enough period with higher ionospheric activity is available. For that reason, ESA has decided to keep the current settings for a longer period (J. van den IJssel, personal communication).

Summarizing, it can be stated that Swarm POD and hl-SST gravity field recovery after October 2015, when all three satellites' tracking loop bandwidths are set to 0.5 Hz or larger, clearly benefits from these updates making additional GPS data screening less critical at least under the condition of relatively low ionospheric activity as currently present. This is of particular relevance for the geodetic community, as Swarm hl-SST solutions thus might contribute even better to fill the gap between the dedicated gravity field missions GRACE and GRACE-FO. Vice versa, when processing Swarm data before October 2015, GPS data screening remains mandatory to obtain best

possible results. By applying an optimized screening threshold taking both ionospheric activity and tracking loop settings into account, the aforementioned drawbacks of the screening might vanish and the gravity solutions might be further improved, but this is beyond the scope of this work and subject to future investigation.

The Swarm kinematic orbits denoted as "original" in this work are available via anonymous ftp at AIUB[2].

Acknowledgements

This work was partly performed in the framework of the Swarm Quality Working Group (QWG), which is organized by ESA. C. Dahle has been funded by the German Federal Ministry of Education and Research (BMBF) with support code 03F0654A. ESA is highly acknowledged for their decision to update the Swarm GPS tracking loop settings during fully operational mode of the mission helping to improve geodetic science results.

References

Basu, S., Groves, K.M., Basu, Su., Sultan, P.J. 2002. Specification and forecasting of scintillations in communication/navigation links: current status and future plans. J. Atmos. Solar-Terres. Phys. 64(16), 1745-1754. http://dx.doi.org/10.1016/S1364-6826(02)00124-4

Beutler, G., Jäggi, A., Mervart, L., Meyer, U. 2010. The celestial mechanics approach: theoretical foundations. J. Geod. 84(10), 605-624. http://dx.doi.org/10.1007/s00190-010-0401-7

Bezděk, A., Sebera, J., Encarnação, J., Klokočník, J. 2016. Time-variable gravity fields derived from GPS tracking of Swarm. Geophys. J. Int. 205, 1665-1669. http://dx.doi.org/10.1093/gji/ggw094

Bock, H., Jäggi, A., Beutler, G., Meyer, U. 2014. GOCE: precise orbit determination for the entire mission. J. Geod. 88(11), 1047-1060. http://dx.doi.org/10.1007/s00190-014-0742-8

[2]ftp://ftp.unibe.ch/aiub/LEO_ORBITS/SWARM/

Buchert, S., Zangerl, F., Sust, M., André, M., Eriksson, A., Wahlund, J.-E., Opgenoorth, H. 2015. SWARM observations of equatorial electron densities and topside GPS track losses. Geophys. Res. Lett. 42, 2088-2092. http://dx.doi.org/10.1002/2015GL063121

Cheng, M., Ries, J. 2016. GRACE Technical Note 07: Monthly estimates of C20 from 5 SLR satellites based on GRACE RL05 models. http://podaac.jpl.nasa.gov/gravity/grace-documentation

Dahle, C., Flechtner, F., Gruber, C., König, D., König, R., Michalak, G., Neumayer, K.-H. 2012. GFZ GRACE Level-2 Processing Standards Document for Level-2 Product Release 0005. Scientific Technical Report STR12/02 - Data, Revised Edition, January 2013, Potsdam, 21 p. http://dx.doi.org/10.2312/GFZ.b103-1202-25

Dobslaw, H., Flechtner, F., Bergmann-Wolf, I., Dahle, C., Dill, R., Esselborn, S., Sasgen, I., Thomas, M. 2013. Simulating high-frequency atmosphere-ocean mass variability for de-aliasing of satellite gravity observations: AOD1B RL05. J. Geophys. Res. Oceans 118(7), 3704-3711. http://dx.doi.org/10.1002/jgrc.20271

Encarnação, J., Arnold, D., Bezděk, A., Dahle, C., Doornbos, E., van den IJssel, J., Jäggi, A., Mayer-Gürr, T., Sebera, J., Visser, P., Zehentner, N. 2016. Gravity field models derived from Swarm GPS data. Earth Planets Space 68:127. http://dx.doi.org/10.1186/s40623-016-0499-9

Flechtner, F., Neumayer, K.-H., Dahle, C., Dobslaw, H., Fagiolini, E., Raimondo, J.-C., Güntner, A. 2016. What Can be Expected from the GRACE-FO Laser Ranging Interferometer for Earth Science Applications? Surv. Geophys. 37(2), 453-470. http://dx.doi.org/10.1007/s10712-015-9338-y

Friis-Christensen, E., Lühr, H., Knudsen, D., Haagmans, R. 2008. Swarm - an earth observation mission investigating geospace. Adv. Space Res. 41(1), 210-216. http://dx.doi.org/10.1016/j.asr.2006.10.008

Hoque, M. M., Jakowski, N. 2008. Estimate of higher order ionospheric errors in GNSS positioning. Radio Sci. 43, RS5008 http://dx.doi.org/10.1029/2007RS003817

Jäggi, A., Bock, H., Prange, L., Meyer, U., Beutler, G. 2011a. GPS-only gravity field recovery with GOCE, CHAMP, and GRACE. Adv. Space Res. 47(6), 1020-1028. http://dx.doi.org/10.1016/j.asr.2010.11.008

Jäggi, A., Meyer, U., Beutler, G., Prange, L., Dach, R., Mervart, L. 2011b. AIUB-GRACE03S. http://icgem.gfz-potsdam.de/ICGEM/

Jäggi, A., Bock, H., Meyer, U., Beutler, G., van den IJssel, J. 2015. GOCE: assessment of GPS-only gravity field determination. J. Geod. 89(1), 33-48. http://dx.doi.org/10.1007/s00190-014-0759-z

Jäggi, A., Dahle, C., Arnold, D., Bock, H., Meyer, U., Beutler, G., van den IJssel, J. 2016. Swarm kinematic orbits and gravity fields from 18 months of GPS data. Adv. Space Res. 57(1), 218-233. http://dx.doi.org/10.1016/j.asr.2015.10.035

Mayer-Gürr, T., Pail, R., Gruber, T., Fecher, T., Rexer, M., Schuh, W.-D., Kusche, J., Brockmann, J.-M., Rieser, D., Zehentner, N., Kvas, A., Klinger, B., Baur, O., Höck, E., Krauss, S., Jäggi, A. 2015. The combined satellite gravity field model GOCO05s. Presentation at EGU 2015, Vienna, April 2015. Geophysical Research Abstracts Vol. 17, EGU2015-12364

Petit, G., Luzum, B. (eds.) 2010. IERS Conventions (2010) (IERS Technical Note No. 36). Frankfurt am Main: Verlag des Bundesamts für Kartographie und Geodäsie, 179 pp., ISBN 3-89888-989-6

Savcenko, R., Bosch, W. 2012. EOT11a - empirical ocean tide model from multi-mission satellite altimetry. DGFI-TUM, Munich, DGFI-Report No. 89. https://mediatum.ub.tum.de/?id=1304935

Sust, M., Zangerl, F., Montenbruck, O., Buchert, S., Garcia-Rodriguez, A. 2014. Spaceborne GNSS-Receiving System Performance Prediction and Validation. In: NAVITEC 2014, 7th ESA Workshop on Satellite Navigation Technologies, ESTEC, Noordwijk, The Netherlands. http://www.cluster.irfu.se/scb/navitec_2014_sus_et_al_final_for_web.pdf

van den IJssel, J., Encarnação, J., Doornbos, E., Visser, P. 2015. Precise science orbits for the Swarm satellite constellation. Adv. Space Res. 56(6), 1042-1055. http://dx.doi.org/10.1016/j.asr.2015.06.002

van den IJssel, J., Forte, B., Montenbruck, O. 2016. Impact of Swarm GPS receiver updates on POD performance. Earth Planets Space 68:85. http://dx.doi.org/10.1186/s40623-016-0459-4

Xiong, C., Stolle, C., Lühr, H. 2016. The Swarm satellite loss of GPS signal and its relation to ionospheric plasma irregularities. Space Weather http://dx.doi.org/10.1002/2016SW001439

Zehentner, N., Mayer-Gürr, T. 2016. Precise orbit determination based on raw GPS measurements. J. Geod. 90(3), 275-286. http://dx.doi.org/10.1007/s00190-015-0872-7